Proceedings World Geothermal Congress 2020+1
Reykjavik, Iceland, April - October 2021

Infrared Spectral Mineralogy for Geothermal Exploration: a Preliminary Study Using Cutting Edge Technology Infrared Imaging Spectroscopy (IRIS)

Kartika P. Savitri[1], Christoph Hecker[1], Freek D. van der Meer[1], Ridwan P. Sidik[2], Marino C. Baroek[2], Herwin Azis[2]

[1]University of Twente, Faculty of Geo-information Science and Earth Observation (ITC) – Hengelosestraat 99, 7514 AE Enschede, the Netherlands

[2]PT Supreme Energy – Menara Sentraya 23rd Floor, Jl. Iskandarsyah Raya No.1A, Kebayoran Baru, Jakarta, Indonesia 12160

k.p.savitri@utwente.nl

Keywords: spectral mineralogy, infrared spectroscopy, infrared imaging spectroscopy, hydrothermal alteration, mineralogy, geology.

ABSTRACT

Infrared spectroscopy is a non-destructive mineralogical analysis with minimum sample treatment required. The mineral identification in this method is based on the energy reflected by molecular vibrational processes upon incoming infrared radiation which is a proxy for mineralogy and mineral chemistry. With this method, we can identify minerals that are difficult to distinguish using some other methods (i.e. methylene blue stain test, binocular microscopy, and petrography), particularly clay minerals which are the important temperature indicator minerals in geothermal systems. Therefore, it is a promising mineralogy analytic method to be applied in geothermal subsurface samples. However, the application of the method in geothermal studies is still limited, especially the recently-developed infrared imaging spectroscopy (IRIS), which is the extension of the conventional (non-imaging) infrared spectroscopy. This paper reviews the current use of infrared spectroscopy for geothermal exploration and present preliminary results of our work using infrared imaging spectroscopy. Our preliminary results show that infrared imaging spectroscopy can identify much more minerals compared to non-imaging infrared spectroscopy, including minerals which are present only in a small amount. Spatial relationships between hydrothermal alteration minerals might be visible in bigger cuttings grains. However, the initial mineral map classification using Spectral Angle Mapper (SAM) shows that it is difficult to determine the threshold which will give an accurate assignment of minerals.

1. INTRODUCTION

Infrared spectroscopy is a non-destructive mineralogical analysis with minimum sample treatment required. It works as a proxy for mineralogy and mineral chemistry. In the short wave infrared (SWIR) range (i.e. 1.3-2.5 micrometres (μm)), the mineral identification is based on the energy emitted by molecular vibrational processes upon incoming infrared radiation (i.e. OH, H_2O, AlOH, FeOH, MgOH and/or CO_3 molecules) (AusSpec International Ltd., 2008). Therefore, this tool works well in identifying hydrothermal alteration products, especially clay minerals . Some of this tool also cover wavelength of visible to near infrared (VNIR - 0.35-1.3 μm) range. The absorption features appear in this range is due to electronic transitions in the iron-bearing minerals (Hunt, 1977; Hunt and Ashley, 1979).

Infrared spectroscopy was first developed for mineral exploration purpose, but later experiments show that it is also applicable for geothermal samples. However, the application of this method in geothermal exploration are still not as extensive as in mineral exploration, especially the recently-developed infrared imaging spectroscopy. The latter technique was demonstrated to produce the more detailed mineralogy identification and visualize them in mineral maps. This paper aims to reviews how infrared spectroscopy has been applied in geothermal exploration as well as introduce the preliminary results of our work using infrared *imaging* spectroscopy on geothermal drill cuttings dataset from one of geothermal fields in Sumatra (Indonesia) belongs to PT Supreme Energy.

2. APPLICATION OF INFRARED SPECTROSCOPY FOR GEOTHERMAL EXPLORATION

2.1 Clay Mineral Identification using Infrared Spectroscopy

Infrared spectroscopy has been applied to identify hydrothermal alteration products for more than 40 years. However, it was firstly used in geothermal studies in 2000s (Yang et al., 2001, 2000). To date, geothermal studies applying this technique have been conducted on both surface and subsurface samples. Along with ammonium mapping, the technique has been used to map the HTA zone on the surface in Acoculco volcanic complex (Canet et al., 2015). It has also been applied to delineate hydrothermal minerals formed in acid environment in New Zealand (Simpson et al., 2006). Infrared spectroscopy has become one of the main tools to identify hydrothermal alteration products in geothermal systems (e.g. Chambefort et al., 2017; Rocha Ruiz & Hernández Zúñiga, 2015) although the less practical XRD analysis is indeed still required to validate the infrared spectroscopy analysis results, especially when the latter is inconclusive.

One of the benefit of the infrared spectroscopy technique is its excellence on identifying clay minerals which is difficult to obtain from other methods (e.g. binocular microscope and petrography). In geothermal systems, clay minerals are important as one of the temperature-indicator minerals, especially illite, interstratified illite-smectite, and smectite. In an undisturbed condition, these minerals do not coexist, Instead, these minerals are precipitated in different temperature range (Browne, 1970, 1978; Reyes, 1990). Therefore, it is essential to distinguish these clay minerals. The spectral distinction between these minerals has been studied by Simpson et al. (2013) using the same clay fraction samples as used in XRD, for validating and quantifying the illite and/or smectite percentage. It was found that illite and smectite correspond to spectra with a hull quotient corrected H_2O/AlOH ratios of >0.96 and <0.76, respectively. The ratio in between corresponds to interstratified illite-smectite of which one of the components is under 80%.

Higher percentage of either smectite or illite will show an overlap H_2O/AlOH ratios with smectite or illite, respectively. Later, it was confirmed by Simpson and Rae (2018) that hull quotient has a better match with XRD results compared to reflectance value. However, the H_2O/AlOH threshold value for these clay minerals in other geothermal systems might be slightly different due to lithology variation and different hydrothermal alteration processes.

Understanding the distribution of low-temperature clay minerals within geothermal systems is essential as this hydrothermal alteration product acts as an impermeable layer enclosing and accumulating heat in the system. The distribution of clay cap is mainly obtained from magnetotelluric (MT) resistivity model marked by resistivity value below 10 ohm-meter (Ωm) (e.g. Arnason et al., 2000; Dyaksa et al., 2016). In order to better understand the relationships between resistivity value and clay mineral distribution, infrared spectroscopy has been applied. The clay characterization obtained from this analysis, combined with additional complementary XRD, was compared to MT resistivity and MeB value (Correa et al., 2013).

The occurrence a clay-rich zone is a sign of high permeability layer, which is also an essential element for a geothermal system. Hydrothermal fluids as an agent for hydrothermal alteration process as well as transferring the heat from the depth to near surface can only pass through permeable layers. Considering that one of the most common permeable features in geothermal systems is fracture, Vidal et al. (2018) introduced a method to locate fracture zones in geothermal system by quantifying clay minerals. The infrared spectra was processed using Gaussian curves approach to quantify the clay minerals. However, this approach is not applicable for mineral identification.

In addition to clay and other hydrothermal minerals, infrared spectroscopy technique was once proposed to also distinguish lithology in subsurface samples (Calvin et al., 2005; Kratt et al., 2004). However, the produced spectra contains mostly a mixture of several minerals in which primary and secondary minerals are difficult to distinguish. Therefore, we can only indicate lithology changes by looking at the general shape of the spectra. Directly identifying the lithology is impractical.

As the recorded spectra is a function of all materials exposed to the instrument, some other materials may have stronger absorption features and thus disguise the hydrothermal mineral features. A number of studies have reported to have impact from non-hydrothermal materials interfering the hydrothermal mineral spectra, including cuttings chip tray (Calvin and Pace, 2016), walnut chips used as additive materials to prevent loss of circulation (Calvin et al., 2010), epoxy glue used to mount drill cuttings (Kratt et al., 2004), drilling mud (i.e. bentonite) (Calvin and Solum, 2005; Littlefield et al., 2012), and volcanic glass (Simpson and Rae, 2018; Simpson et al., 2013). Walnut chips has a strong absorption features of organic materials and thus it is easy to distinguish from minerals. Likewise, epoxy glue spectra is easy to observe as it has the 1.7 µm feature which is uncommon in minerals (Kratt et al., 2004). However, drilling mud and volcanic glass have similar absorption features to smectite causing the interpretation of the latter mineral less accurate.

2.2 Expansion of the Practice

Although infrared spectroscopy is excellent for identifying hydrothermal minerals, the technique can only detects dominant and/or more spectrally active minerals (Calvin and Pace, 2016). Moreover, it is more likely that the spectra contains mixtures of minerals in which identifying its endmember minerals is challenging. Up until now, there have been several studies proposing different approaches on using the infrared spectroscopy data in order to optimize its usage and meaning on understanding geothermal systems.

In 2010, a graphical and statistical processing method is suggested to automatically and objectively identify minerals by clustering the normalized reflectance spectra. The method is meant to minimize the need of XRD validation (Canet et al., 2010). However, the proposed method has not been widely adapted. Other infrared spectral mineralogy studies still adopt manual identification by visually comparing the spectra with existing spectral library.

Another statistical-based approach is demonstrated by Littlefield et al. (2012). The approach is applied to remove noise and spatially reduced the data which is intended to focus on spectrally unique pixels only. In this study, additional approach was also undertaken to derive thresholded mineral classification results. From these results, spectral-derived hydrothermal alteration logs were created. It was demonstrated that these logs are useful as a scanning tool for further and more detail mineralogy and mineral paragenesis study using other analysis methods.

The most important benefit of having hydrothermal alteration logs is that it becomes easier to observe the changes on hydrothermal alteration products within a well. In that way, we can easily see the temperature changes based on the distribution of temperature-indicator minerals. In order to produce a complete log, high vertical resolution data is needed. Since infrared spectra acquisition is fast, data acquisition in a high vertical resolution is accessible as demonstrated by Calvin et al. (2010). In addition to high vertical resolution data acquisition, there was a processing method developed by Calvin and Pace (2016) for producing hydrothermal alteration logs comparable to geophysical logs.

The most recent development of infrared spectroscopy technique is infrared imaging spectroscopy (IRIS). Similar to the conventional (i.e. non-imaging) infrared spectroscopy, IRIS detects minerals based on the energy reflected by molecular vibrational processes upon incoming infrared radiation. The difference of IRIS is that it does not only produces a single spectrum, but also visualization of the samples. With this method, we can obtain the visualization of the sample and at the same time obtain a spectrum for every pixel of the scanned images. In that way, we can identify less common minerals in cuttings as long as they (spectrally) dominate at least a pixel in IRIS images. Previous studies in mineral exploration have demonstrated that the technique can produce a map of hydrothermal alteration minerals within the scanned samples (Mathieu et al., 2017; Taylor, 2000). Thus, it is easier to create hydrothermal mineral logs using IRIS.

IRIS was first used in a geothermal application by Kraal et al. (2018) showing that IRIS see less mixture than the non-imaging infrared spectroscopy and thus identify minerals more accurately than the non-imaging infrared spectroscopy. Since it has not been widely applied, the technique still require testing on real case geothermal systems. Therefore, we have initiated a project applying IRIS on geothermal drill cuttings dataset from one of geothermal fields in Sumatra.

3. OUR PROJECT

3.1 Samples and Methods

We have run our first test using IRIS on our drill cuttings dataset. Samples were washed prior to being analysed to remove the remaining drilling muds. Image and spectral data were acquired using labscanner 100x50 imaging station equipped with hyperspectral SWIR camera manufactured by Specim Spectral Imaging Ltd. The instrument measures shortwave infrared light (1.0 – 2.5 µm) in 288 spectral bands and 384 spatial pixels. Original aluminium cups (i.e. not painted) were used as sample tray. We found that the cup was very reflective and thus interfere our sample spectra on the outside edge of the sample area. Observation on individual image has been undertaken to define the masking area as each sample has different amount as well as different interfere results from the cup. Dark pixel masking using band threshold to Region of Interest (ROI) was added selecting only spectra which has a value above 0.15 at 1.6027 µm in order to remove noisy pixels which we thought is related to the natural dark coloration of the lithology.

Mineral identification was done by visually observing minimum wavelength maps. These maps visualise the position and depth of the deepest absorption feature in a certain wavelength range (Hecker et al., 2019; Kokaly et al., 2017; Van Ruitenbeek et al., 2014). Different wavelength position is indicated by different colour, whereas depth is reflected by brightness level where maximum brightness marks the deepest feature. In our work, the maps were created in seven different wavelength ranges (Table 1). Each range were created to target absorption features of different molecules. 23 endmember were identified manually from wavelength maps based on different colour patterns with maximum brightness indicating deepest features occur at different wavelength position. These endmember were then used to classify the images and produce mineral maps using Spectral Angle Mapper (SAM) approach. The approach used different threshold setting for each endmembers which were defined from a number of experiments on several samples.

Table 1: Wavelength ranges used for creating wavelength maps along with their targeted feature(s)

No	Wavelength range	Targeted feature(s)
1	1.35-1.55 µm	H_2O, OH
2	1.84-1.95 µm	H_2O, OH
3	2.1-2.23 µm	Al-OH
4	2.195-2225 µm	Al-OH
5	2.22-2.3 µm	Fe-OH
6	2.29-2.4 µm	Mg-OH, CO_3
7	2.33-2.355 µm	Mg-OH, CO_3

3.2 Initial Results

3.2.1 Identified Minerals

From wavelength maps investigation, we identified 23 endmember materials including16 pure endmember minerals, 6 mixtures of minerals, and 1 spectrum of organic material. The latter spectra belongs to sawdust which is used as lost-circulation materials (LCM) or additive materials to prevent from loss of circulation. The mineral mixtures spectra were also selected and used for the classification in order to get a better estimation of the mineral abundance. The pure endmember minerals identified include dickite, montmorillonite, nontronite, chlorite, opal, prehnite, epidote, calcite, ankerite, gypsum, two zeolite spectra, and three unknown spectra (Figure 1).

There are four clay minerals present in the samples (Figure 1a). Two of them are smectite members, namely montmorillonite and nontronite. Montmorillonite is characterised by its Al-OH absorption feature at ~2.203 µm, while nontronite is characterised by its Fe-OH absorption feature at ~2.287 µm. Illite is characterized by having Al-OH absorption features at ~2.209 µm and ~2.349 µm. The latter feature is absent in montmorillonite. Meanwhile, dickite is the only endmember showing a doublet of Al-OH feature at 2.180 and 2.203 µm and a doublet of OH feature at 1.383 µm and at 1.411 µm.

Chlorite is also present characterised by Fe-OH/Mg-OH feature at ~2.259 µm and ~2.348 µm. Opal has been observed in previous studies (Calvin et al., 2010; Calvin and Pace, 2016; Canet et al., 2015) for having absorption features at 1.43, 1.92, and 2.20 µm where the last feature distinguishing opal from hydrated quartz. In our samples, the opal spectra has features at ~2.208 and ~2.292 µm in addition to the 1.4 and 1.9 water features. A few of them shows a clear distinction between the ~2.208 and ~2.292 µm feature, but most of the spectra have these two features as one broad feature. Prehnite is characterised by unusual OH feature at ~1.48 µm together with three features at ~2.23, ~2.28, and ~2.35 µm. The epidote spectra of our samples shows a strong ~2.25 and ~2.34 µm feature. The ~1.54 µm diagnostic feature of epidote is also present. However, there are a few traces of illite reflected in the epidote spectra (e.g. the ~1.41 and the ~1.91 µm feature of illite resulting in the asymmetric and broad ~1.9 feature in the spectra).

There are two carbonate minerals present in our samples, namely calcite and ankerite. In infrared spectra, carbonate minerals are characterized by the ~2.34 µm CO_3 feature. However, this feature is weak in ankerite. Instead, ankerite spectra shows a big broad trough centred at ~1.36 µm which is the artefact of a strong Fe^{2+} feature. Gypsum is characterized by OH-sulfate feature at ~1.75 µm and multiple water features at ~1.4 and ~1.9 µm. Zeolite group is also characterized by multiple water absorption at ~1.4 and ~1.9 µm, but it does not have the ~1.7 µm OH-sulfate feature. Instead, it has a feature at ~1.15 µm. We distinguished two zeolite spectra in our samples by their ~1.15 µm feature. The feature is obvious in one zeolite spectra, but absent in the other. Assigning these zeolite spectra to a particular zeolite mineral is difficult.

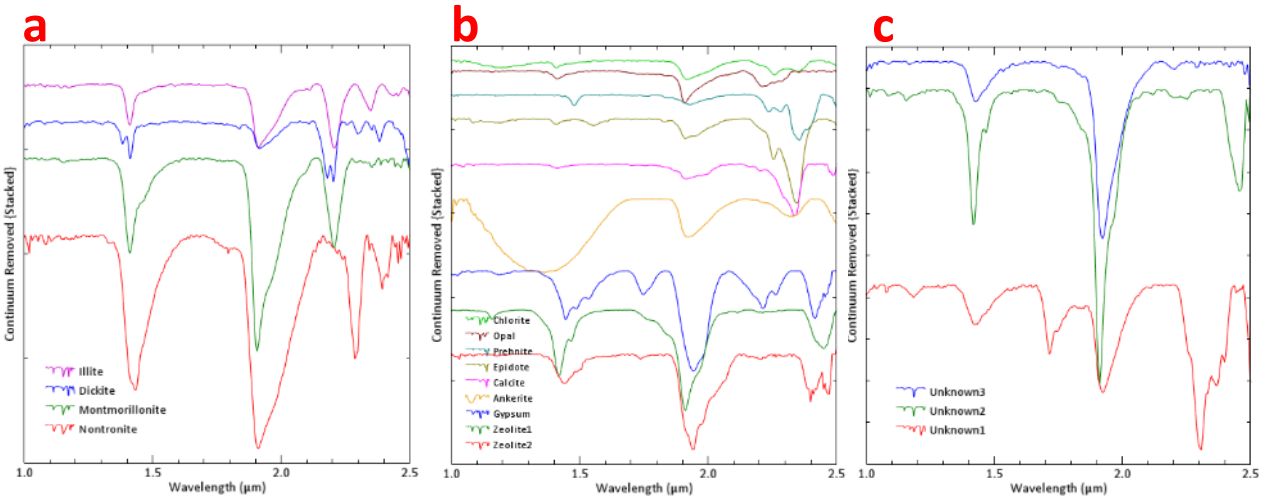

Figure 1: Spectra of the pure endmember minerals identified in our samples: (a) clay minerals; (b) non-clay minerals; (c) unidentified spectra.

There are three spectra from our samples that are still not assigned to any particular mineral yet (Figure 1c). One of these spectra shows a multiple water features at ~1.4 and ~1.9 µm as well as an absorption feature at ~1.71 µm which possibly a OH-sulfate feature (i.e. Unknown1). This spectra also has a multiple absorption feature at ~2.3 µm. The other two unassigned spectra is similar to each other by having only the ~1.41 µm and 1.91 µm features yet the shape of these features are different. In one of the spectra (i.e. Unknown3), both features have a broader shape. On the other hand, the other spectra (i.e. Unknown2) shows a deep and sharp features at both wavelength positions an another feature at ~2.45 µm.

3.2.2 Mineral map classification

In general, the SAM classification. Results from four samples are presented in this paper (Figure 2). According to our SAM results, the composition of these four samples are as follows:

- ESA-01/0057-0060m: dickite-montmorilonite mixture (45.92%), opal (32.57%), montmorillonite-illite mixture (9.95%), LCM (5.59%), montmorillonite (2.89%), illite (1.55%), zeolite1 (0.46%), montmorillonite-chlorite mixture (0.42%), gypsum (0.25%), nontronite (0.17%), zeolite2 (0.07%), illite-chlorite mixture (0.07%), nontronite-dickite mixture (0.04%), chlorite (0.04%), dickite (0.03%)
- ESA-01/0261-0264m: montmorillonite (60.73%), zeolite1 (11.62%), opal (11.45%), montmorillonite-illite mixture (10.09%), dickite-montmorilonite mixture (2.04%), gypsum (1.65%), LCM (1.36%), zeolite2 (0.70%), montmorillonite-chlorite mixture (0.29%), illite (0.06%), nontronite (0.01%), illite-chlorite mixture (0.09%), chlorite (0.04%)
- ESA-01/0522-0525m: illite-chlorite mixture (31.36%), montmorillonite-chlorite mixture (28.68%), illite (26.85%), chlorite (4.85%), opal (4.29%), montmorillonite-illite mixture (0.86%), dickite-montmorilonite mixture (0.68%), zeolite1 (0.51%), montmorillonite (0.39%), unknown2 (0.13%), calcite (0.11%), zeolite2 (0.10%), gypsum (0.08%), epidote (0.06%), prehnite-chlorite mixture (0.06%)
- ESA-02/0663-0666m: montmorillonite-chlorite mixture (29.66%), opal (19.17%), illite (18.31%), montmorillonite-illite mixture (13.98%), illite-chlorite mixture (6.48%), LCM (5.60%), dickite-montmorilonite mixture (5.17%), chlorite (0.87%), calcite (0.45%), zeolite1 (0.15%), zeolite2 (0.09%), montmorillonite (0.04%), prehnite-chlorite mixture (0.03%), unknown2 (0.03%)

In our samples, there is a limitation caused by their naturally dark-coloured lithology resulting in a significant amount of masked pixels as well as unclassified spectra. The abundance of minerals listed above were calculated by excluding these masked and unclassified pixels. Some samples show only a limited number of classified pixels (not presented here). An initial presumption is that a low percentage of classified pixels may suggest low intensity of alteration.

4. DISCUSSION

IRIS method allows us to visually observe the distribution of hydrothermal minerals in the samples. From three ESA-01 samples (Figure 2a-c), we can see the changes of mineralogy within 500 m depth in this well. Not only that, we can also calculate the abundance of each minerals. Minerals present below 1% are also detected using this technique which is difficult in other mineralogy analytic methods. Especially for drill cuttings samples, IRIS allows us to scan the entire cuttings samples, whereas other methods can only use a small part of the samples either to be prepared in a grain mount or powder. Consequently, we will not miss identifying any minerals easily using this technique, except for non-spectrally active minerals.

In addition to mineral distribution, we may also see the spatial relationships between minerals. In ESA-01/0522-0525m sample (Figure 2c), there are a few grains showing halo in which the mineralogy of the edge and middle part are different. Such spatial relationships is hardly shown in other samples. This might due to the size of the cuttings chips in ESA-01/0522-0525m sample which are generally bigger than in other sample so that they expose more minerals including clearly capture their spatial relationships.

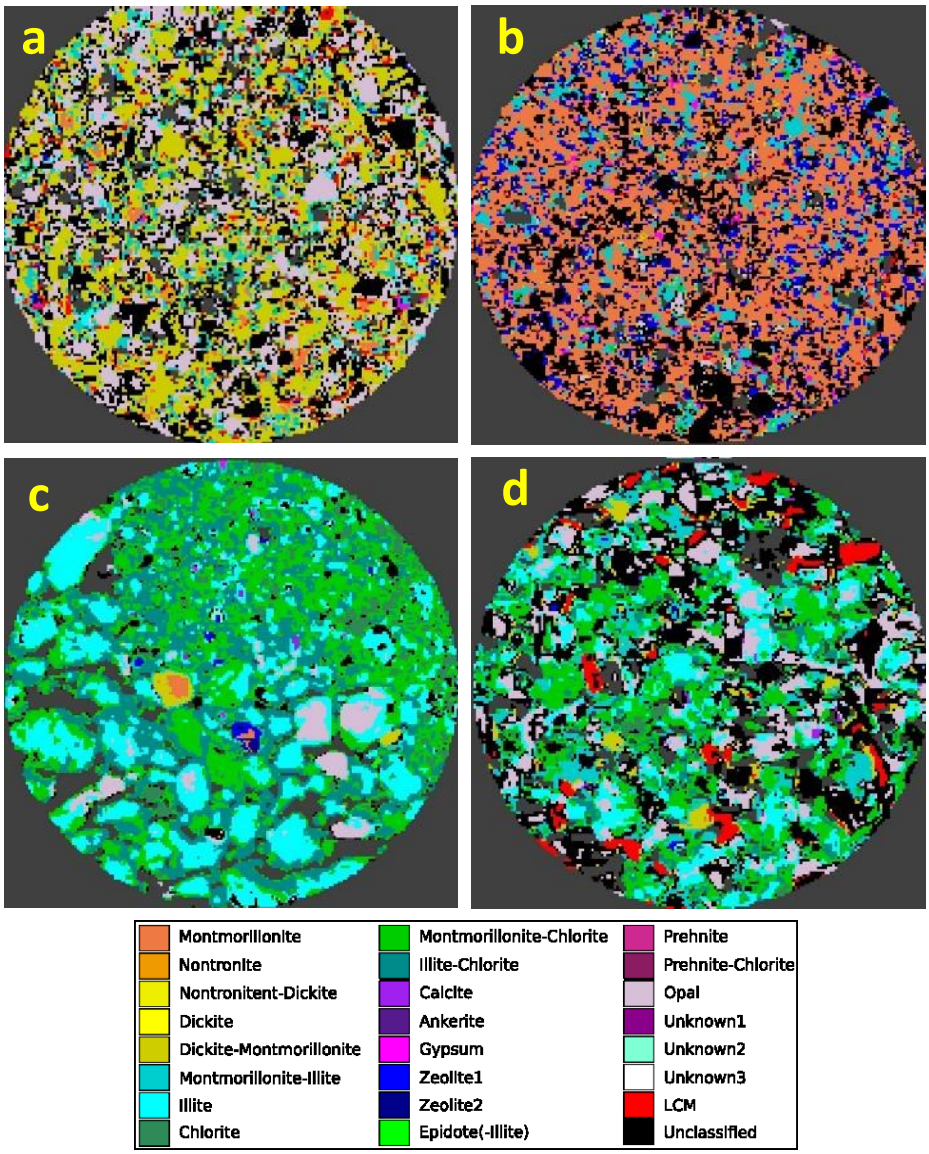

Figure 2: Mineral maps of the samples created using SAM: (a) ESA-01/0057-0060m; (b) ESA-01/0261-0264m; (c) ESA-01/0522-0525m; (d) ESA-02/0663-0666m. Sample code represents well number/depth range. Colour are as explained in the legend, except grey colour representing masked pixels.

Manual validation (i.e. visually comparing the SAM-assigned endmember mineral with the spectra) has been done on a limited number of samples, showing that SAM has correctly assigned most of the minerals using the current threshold settings. However, there is still some pixels that were not assigned correctly. This issue mostly arise from mixture endmembers, e.g. illite-chlorite mixture. The mixture can be easily distinguished (i.e. in manual interpretation by an operator) from montmorillonite-chlorite mixture by the proportion of ~1.91 µm water feature compared to the ~2.20 µm and ~2.35 µm features. The illite-chlorite mixture has all of the three features at about the same depth (Figure 3, red spectrum), whereas montmorillonite-chlorite mixture has a significantly deeper water feature than the other two features (Figure 3, dark green spectrum). Random selection on pixels assigned as illite-chlorite mixture in Figure 2d shows spectra that is more comparable to montmorillonite-chlorite mixture (Figure 3). This may be because SAM classification works based on algorithm which try to match and fit the entire spectra or a range of the spectra. We cannot easily set the classifier to only focus on the diagnostic features of each endmembers.

Threshold settings of each inputted endmember minerals determine how full the spectra would be matched and fitted by SAM. In this work, a visual preliminary observation was undertaken to determine the threshold. During the threshold determination process, we found that it is time consuming and difficult to determine accurate global threshold settings for the entire sample set. As far as we observed, there would always be some samples showing an anomaly where most samples works on a certain threshold setting. For example, with a threshold of 0.1 radian, we get a well-suited zeolite assignment in most of our samples but we also get a number of montmorillonite being assigned as zeolite in several samples including ESA-01/0261-0264m (Figure 2b). In other test, we used smaller threshold but that made many zeolite pixels were unclassified. This observation shows that smaller threshold leads to missing some information in several samples while higher threshold solve this issue but gives some wrong results in other samples.

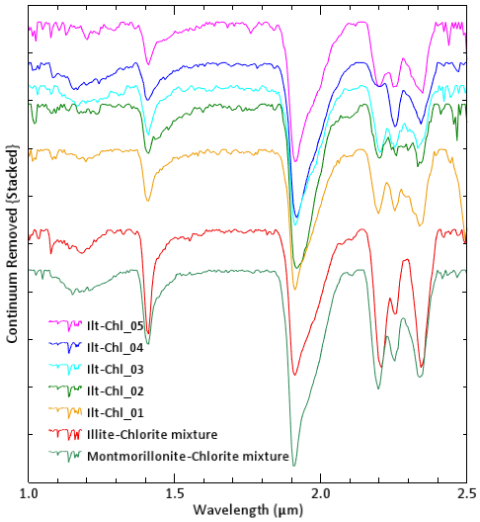

Figure 3: Spectra of five pixels assigned as illite in SAM-derived mineral maps of ESA-02/0663-0666m (illite-chlorite mixture_01-05) compared to the illite-chlorite and montmorillonite-chlorite mixture spectra used as the input for the classification.

5. SUMMARY AND FUTURE PROJECT GOALS

Infrared imaging spectroscopy can identify minerals even at low percentage. Depending on the size of cuttings chips, spatial relationships between hydrothermal alteration minerals might be visible. However, mineral identification using Spectral Angle Mapper (SAM) classification works based on algorithm which try to match and fit the entire spectra. The results strongly depend on the threshold settings of each inputted endmembers. Results of our preliminary works express that SAM shows a lot of limitation which consequently leads to produce less accurate mineral maps and mineral abundance estimation. For future works, we would like to apply knowledge-based classification approach, such as decision-tree to mimic the decisions taken by a trained operator. Furthermore, more samples will be scanned and analysed. Other mineralogy analytical results (e.g. petrography and X-ray diffractometry – XRD) will also be undertaken to validate the IRIS results.

ACKNOWLEDGEMENT

This work is part of the collaborative research project between University of Twente and PT Supreme Energy through the Indonesia–Netherlands Geothermal Capacity Building Programme (GEOCAP).

REFERENCES

Arnason, K., Karlsdottir, R., Eysteinsson, H., Flovenz, O. G., and Gudlaugsson, S. T.: The Resistivity Structure of High-Temperature Geothermal Systems in Iceland, *Proceedings of the World Geothermal Congress*, (2000), 923–928.

AusSpec International Ltd.*GMEX Volume 1: Spectral Interpretation Field Manual*, (2008). Australia: AusSpec International Ltd.

Browne, P. R. L.: Hydrothermal alteration as an aid in investigating geothermal fields, *Geothermics*, **2**(PART 1), (1970), 564–570.

Browne, P. R. L.: Hydrothermal Alteration in Active Geothermal Fields, *Annual Review of Earth and Planetary Sciences*, **6**(1), (1978), 229–248.

Calvin, W., Kratt, C., and Faulds, J.: Infrared spectroscopy for drillhole lithology and mineralogy, *… , Thirtieth Workshop on …*, (2003), (2005), 2–6.

Calvin, W., Lamb, A., and Kratt, C.: Rapid Characterization of Drill Core and Cutting Mineralogy using Infrared Spectroscopy, *Transactions - Geothermal Resources Council*, **34**, (2010), 5.

Calvin, W. M., and Pace, E. L.: Mapping alteration in geothermal drill core using a field portable spectroradiometer, *Geothermics*, **61**, (2016), 12–23.

Calvin, W. M., and Solum, J. G.: Drill Hole Logging with Infrared Spectroscopy, *Geothermal Resources Council Transactions*, **29**, (2005), 565–568.

Canet, C., Arana-Salinas, L., González-Partida, E., Pi Puig, T., Prol Ledesma, R. M., Franco, I., … López-Hernández, A.: A statistics-based method for the short-wave infrared spectral analysis of altered rocks: An example from the Acoculco Caldera, Eastern Trans-Mexican Volcanic Belt, *Journal of Geochemical Exploration*, **105**, (2010), 1–10.

Canet, C., Hernández-Cruz, B., Jiménez-Franco, A., Pi, T., Peláez, B., Villanueva-Estrada, R. E., … Salinas, S.: Combining ammonium mapping and short-wave infrared (SWIR) reflectance spectroscopy to constrain a model of hydrothermal alteration for the Acoculco geothermal zone, Eastern Mexico, *Geothermics*, **53**(53), (2015), 154–165.

Chambefort, I., Lewis, B., Simpson, M. P., Bignall, G., Rae, A. J., and Ganefianto, N.: Ngatamariki geothermal system: Magmatic to epithermal transition in the taupo volcanic zone, New Zealand, *Economic Geology*, **112**(2), (2017), 319–346.

Correa, N. A., Rae, A., and Sepulveda, F.: Distribution of clay minerals through a Conductive (MT) zone on the margins of a high-temperature geothermal reservoir, Wairakei Geothermal Field, Taupo Volcanic Zone, New Zealand, *Transactions - Geothermal Resources Council*, **37**, (2013), 459–462.

Dyaksa, D., Ramadhan, I., and Ganefianto, N.: Magnetotelluric Reliability for Exploration Drilling Stage: Study Cases in Muara Laboh and Rantau Dedap Geothermal Project, Sumatera, Indonesia, *Proceedings of the 41st Workshop on Geothermal Reservoir Engineering*, (2016). Stanford, California.

Hecker, C., van Ruitenbeek, F. J. A., van der Werff, H. M. A., Bakker, W. H., Hewson, R. D., and van der Meer, F. D.: Spectral Absorption Feature Analysis for Finding Ore: A Tutorial on Using the Method in Geological Remote Sensing, *IEEE Geoscience and Remote Sensing Magazine*, **7**(2), (2019), 51–71.

Hunt, G. R.: Spectral signatures of particulate minerals in the visible and near infrared, *Geophysics*, **42**(3), (1977), 501–513.

Hunt, G. R., and Ashley, R. P.: Spectra of altered rocks in the visible and near infrared, *Economic Geology*, (74), (1979), 1613–1629.

Kokaly, R., Graham, G. E., Hoefen, T. M., Kelley, K. D., Johnson, M. R., Hubbard, B. E., and Buchhorn, M.: Multiscale Hyperspectral Imaging of the Orange Hill Porphyry Copper Deposit, Alaska, USA, with Laboratory-, Field-, and Aircraft-based Imaging Spectrometers, *Proc. of the Sixth Decennial International Conference on Mineral Exploration*, (2017), 923–943.

Kraal, K., Ayling, B., Calvin, W., and Browning, D.: Comparison of a portable field spectrometer and automated imaging on geothermal drill core: A pilot study, *Transactions - Geothermal Resources Council*, **42**, (2018), 1327–1339.

Kratt, C., Calvin, W., and Lutz, S. J.: Spectral Analyses of Well Cuttings from Drillhole DP23-1, Desert Peak EGS Area, Nevada -- Preliminary Study of Minerals and Lithologies by Infrared Spectrometry, *Transactions - Geothermal Resources Council*, **28**, (2004), 473–476.

Littlefield, E., Calvin, W., Stelling, P., and Kent, T.: Reflectance spectroscopy as a drill core logging technique: An example using core from the Akutan, *Transactions - Geothermal Resources Council*, **36**, (2012), 1281–1283.

Mathieu, M., Roy, R., Launeau, P., Cathelineau, M., and Quirt, D.: Alteration mapping on drill cores using a HySpex SWIR-320m hyperspectral camera: Application to the exploration of an unconformity-related uranium deposit (Saskatchewan, Canada), *Journal of Geochemical Exploration*, **172**, (2017), 71–88.

Reyes, A. G.: Petrology of Philippine geothermal systems and the application of alteration mineralogy to their assessment, *Journal of Volcanology and Geothermal Research*, **43**(1–4), (1990), 279–309.

Rocha Ruiz, D. A., and Hernández Zúñiga, R.: Distribution of Hydrothermal Alteration in the Cerritos Colorados Geothermal Field, Mexico, *Transactions - Geothermal Resources Council*, **39**, (2015).

Simpson, M. P., Mauk, J. L., Bowyer, D., and Worland, R. J.: Alteration mineral studies of an epithermal prospect and a geothermal field using the TerraSpec, *Proceedings of the 39th Annual Conference of the New Zealand Branch of the AusIMM*, (2006), 247–256.

Simpson, M. P., and Rae, A. J.: Short-wave infrared (SWIR) reflectance spectrometric characterisation of clays from geothermal systems of the Taupō Volcanic Zone, New Zealand, *Geothermics*, **73**, (2018), 74–90.

Simpson, M. P., Rae, A. J., Ganefianto, N., and Sepulveda, F.: Short wavelength infrared (SWIR) spectral characterisation of smectite, illite-smectite and illite for geothermal fields of the Taupo Volcanic Zone, New Zealand, *Proceedings of the 35th New Zealand Geothermal Workshop*, (2013), 17–20. Rotorua, New Zealand.

Taylor, G. R.: Mineral and lithology mapping of drill core pulps using visible and infrared spectrometry, *Natural Resources Research*, **9**(4), (2000), 257–268.

Van Ruitenbeek, F. J. A., Bakker, W. H., Van Der Werff, H. M. A., Zegers, T. E., Oosthoek, J. H. P., Omer, Z. A., … Van Der Meer, F. D.: Mapping the wavelength position of deepest absorption features to explore mineral diversity in hyperspectral images, *Planetary and Space Science*, **101**, (2014), 108–117.

Vidal, J., Glaas, C., Hebert, B., Patrier, P., Beaufort, D., and Genter, A.: Use of SWIR spectroscopy for the exploration of permeable fracture zones in geothermal wells at Rittershoffen (Alsace, France), *Transactions - Geothermal Resources Council*, (2018).

Yang, K., Browne, P. R. L., Huntington, J. F., and Walshe, J. L.: Characterising the hydrothermal alteration of the Broadlands-Ohaaki geothermal system, New Zealand, using short-wave infrared spectroscopy, *Journal of Volcanology and Geothermal Research*, **106**(1–2), (2001), 53–65.

Yang, K., Huntington, J. F., Browne, P. R. L., and Ma, C.: An infrared spectral reflectance study of hydrothermal alteration minerals from the Te Mihi sector of the Wairakei geothermal system, New Zealand, *Geothermics*, **29**(3), (2000), 377–392.